JOURNAL OF Applied Polymer SCIENCE

Preparation of PTT/Clay Nanocomposites with Solid-State Polymerized Polytrimethylene Terephthalate

G. Engelmann, E. Bonatz, J. Ganster, M. Pinnow, A. Bohn
Department of Material Development and Structure Characterization, Division Biopolymers, Fraunhofer—Institute of Applied Polymer Research, Geiselbergstraße 69 14476 Potsdam-Golm, Germany
Correspondence to: G. Engelmann (E-mail: Gunnar.Engelmann@iap.fraunhofer.de)

ABSTRACT: To enhance the effectiveness of polytrimethylene terephthalate (PTT) for the preparation of clay-based nanocomposites by melt intercalation and to upgrade the mechanical performance of these materials, solid-state-polymerization (SSP) experiments with neat PTT were carried out at 190, 200, and 210°C prior compounding to increase the average molecular weight and, based on this, the melt viscosity of this polymer. The progress of SSP was registered by time dependent sampling of intrinsic viscosity data. From this, activation energy of 180.6 kJ mol^{-1} was calculated. A characteristic sublimate formed during these SSP-reactions was identified by mass-spectroscopy to be a mixture of cyclic oligomers containing 2, 3, 4, and 5 monomeric units. The melt viscosity of neat PTT(SSP) could be increased from $\sim$ 460 to 15,000 Pa s^{-1}. Therefore, tensile strength and Young's modulus were improved by 3.5 and 9%, respectively. Manufacturing of PTT(SSP) and the modified nanoclay was carried out with a corotating twin-screw-extruder at 230°C. A concentration of 3% of the inorganic filler component in the composites was aimed at. Compared with the data of virgin PTT, tensile strength, and modulus of the PTT(SSP)-based nanocomposites could be enhanced by $\sim$ 9 and 40%, respectively. Additionally, a SSP-reaction of the nanocomposite prepared with non-pretreated PTT and nanoclay was performed at 210°C to test the robustness of the matrix polymer PTT against the influences of the nanofiller. © 2012 Wiley Periodicals, Inc. J. Appl. Polym. Sci. 000: 000–000, 2012

KEYWORDS: solid-state polymerization; polyesters; clay; nanocomposites; extrusion

Received 14 April 2011; accepted 15 February 2012; published online 00 Month 2012
DOI: 10.1002/app.37501

INTRODUCTION

Nanocomposites are still in the focus of research activities. From the point of view of processing, dispersing of the fillers in the polymer matrix is dominated by melt intercalation.[1] The repertoire of the matrix polymers used is extensive.[2,3] Beside bio-based polymers like PLA,[4] PHB,[5] and starch[6] the main focal point of interest is on synthetic polymers like polyamide 6,[7] polypropylene,[8] polyethylene,[9] polystyrene,[10] polycarbonate,[11] further polyamides,[12] polyurethane,[13] or aromatic polyesters like PET, PBT, and PTT,[14–16] for instance.

In the last years, a special development for aromatic polyesters becomes apparent. In the past, the polyester markets were dominated by polyethylene terephthalate (PET) and polybutylene terephthalate (PBT). Owing to their individual properties, PET was mostly processed to bottles, films[17] and fibers.[18] In contrast, PBT applications were mainly found in the electrical and automotive industries.[19] Contrary to PET and PBT, manufacturing of polytrimethylene terephthalate (PTT) was not efficient because 1,3-propanediol (PDO) was too expensive, compared with 1,2-ethanediol or 1,4-butanediol. Progress in the production of 1,3-propanediol cleared the way for PTT to the market. Shell-company produces PDO based on a chemical process and distributes the corresponding PTT with the trade name Corterra.[20] In contrast, DuPont developed a bio-based process whereby PDO can be derived from corn sugar by fermentation. DuPont brought the PTT-based products labeled Sorona to the market.[21]

Manufacturing of PTT can be performed by melt polycondenzation of PDO with terephthalic acid (TPA) or dimethyl terephtalate (DMT).[22–24] The first step means esterification of TPA with 1,3-propanediol or transesterification of DMT with PDO. In a second step, the resulting intermediates are subjected to polycondenzation in vacuum until the desired molecular weight is reached.

The application of PTT is mainly focused on fibers due to their softness and colorability.[25] Additionally, PTT fiber would combine the good resiliency and bulk of nylons with the inherent stain resistance and low static generation of PET.[26]

Different attempts were made to establish PTT as an engineering plastic. Kim et al. published about the application of solid-state polymerization (SSP) to PTT starting with the commercially available polyesters Corterra and Sorona to get very high molecular weight PTT (M_w = 110,000 g mol^{-1}).[27] During SSP, the polymer has to be thermally treated below the melting point and above the glass-transition temperature. Then, polycondenzation restarts without polymer melting. Specific reaction problems like the influence of diffusion of by-products out of the granules or the influence of the granule size on the reaction kinetic, for instance, were studied for aromatic polyesters.[28–31] Duh[32] highlighted the efficiency of a simplified mathematical model to analyze the kinetic SSP-parameters of PTT.

The preparation of composites is another strategy to establish PTT as an engineering plastic. Various fibers were used as reinforcing agents for PTT-based composites.[33,34] The application of nanofillers for the preparation of nanocomposites is another way to upgrade the performance of PTT. The properties of nanocomposites are partly determined by the chemical and geometrical structures of the nanofillers. Nanoparticles with huge aspect ratios like layered silicates, double-layered hydroxides or carbon nanotubes offer the chance for better mechanical properties, barrier properties or, for the carbon fillers, electrical conductivity.[35–37] Organically modified layer-structured clays (OMC) are economically interesting. Their chemical modification is possible by the exchange of the small inorganic cations against bigger alkylated ammonium-,[38,39] imidazolium-,[40] and phosphonium-[41] cations, with a benefit for alkylated ammonium salts. As a result, the distances between the galleries of the clays increase[42] and the contact between the platelets and the matrix can be adapted.[43] From an industrial perspective, melt compounding of OMC by extrusion is a very attractive method to prepare such nanocomposites.[44] Filler dispersing and platelet exfoliation profit from high viscosity of the polymer melts. In general, the resistance of aromatic polyesters is limited with respect to intensive impact of heat, especially in combination with mechanical stress. Therefore, polyester degradation has to be expected during extrusion, preferably at higher speeds of rotation.[45] Manufacturing of aromatic polyesters like PET, PTT, and PBT in the presence of organically modified clays forces degradation of the polyesters.[46,47] Polymer degradation lowers polymer melt viscosity and works counterproductive with respect to the preparation of OMC-nanocomposites by melt compounding.

The application of high-molecular SSP-treated PTT is an interesting aspect for the preparation of OMC-based nanocomposites to upgrade the performance of PTT. Despite the danger that the degree of degradation of high-molecular polyesters during extrusion can be higher than that of low-molecular PTT,[48] platelet exfoliation could profit from an excess of melt viscosity of PTT(SSP) especially at the beginning of melt compounding. However, if the final molecular weight of PTT(SSP) after processing should be higher than that of the corresponding PTT-reference, compounded under comparable conditions, then additional positive effects for the material properties of the PTT(SSP)-based composites can be expected.

The main objective of this work is the preparation of PTT(SSP)-based nanocomposites via melt compounding according to the experiments described in Ref. [47]. To improve material properties and to support intercalation and exfoliation of an organically modified MMT, a high-molecular PTT(SSP) has to be separately prepared by solid-state polymerization of commercially available PTT prior to compounding. The average molecular weight of this PTT(SSP) should be higher than that published by Kim.[27] To complete the concept, selected results for a postcompounding SSP of a PTT-based nanocomposite are presented.

Beside standard methods to identify exfoliated platelets in the composite matrix like X-ray and TEM investigations, a combination between SEM and plasma etching is presented.

EXPERIMENTAL

Materials

PTT (26 ± 2 mg per pellet) was used as purchased from PTT Poly Canada. Sample of modified clay Nanofil 2 (bentonite modified with benzyldimethylstearylammonium cations) was used as ordered from SüdChemie, Germany.

Sample Preparation

Solid-State-Polymerization (SSP). The apparatus for the SSP-experiments was an evaporation rotator adapted to the conditions of SSP-experiments. A 2-L round flask was loaded with 350 g of dried pellets and tempered in a salt bath at 190, 200, and 210°C for 30–35 h under rotation. The flask was evacuated by vacuum (11 ± 3 mbar) and a gentle flow of nitrogen of 3 L h^{-1} through the flask protected the pellets against oxidation by oxygen and supported the diffusion of molecular condensation products from the pellets out of the flask. After a preselected time sequence, samples were removed from the flask for analysis.

Extrusion. At first a corotating Leistritz-double screw extruder ZSE 18HP with a cooled feeder and nine separately heatable blocks is used. A heatable nozzle/jet panel and the 3-mm round nozzle are joined to block nine. The temperatures for all heating blocks of the extruder were adjusted to 230–240°C. One degassing top each with one oil pump each are joined to blocks 5 and 8. With a good seal, a vacuum of <1 mbar could be reached. The dosing into the feeder was done volumetrically over a color-exact-dosing instrument by dosing screw-tube combinations that were adapted to material and output by adjusting the dosing-screw rotation. Powders were mixed in a Turbula-mixer with milled PTT. All materials were dried at 130°C for 7 h before use. To minimize decomposition due to thermo-oxidation, storage tanks and dosing instruments were rinsed with 200 L h^{-1} nitrogen.

After cooling in water bath granulation began. Cylindrical particles 1.5–2 mm in diameter and 3–4 mm in length were obtained.

Injection Molding. All materials, neat polymers and composite pellets, were dried at 130°C for 7 h before injection molding with a BOY 22A in combination with the control panel Procan CT. The temperatures of the separable heating zones were 70°C

(enter), 230°C (zone 1), 240°C (zone 2), 245°C (zone 3), and 245°C (nozzle). The clamping force was 220 kN.

Instrumentation

Elementary Analysis. EA 1110 (CE INSTRUMENTS) used Dynamic Flash Combustion, gas chromatographic column (Porapak PQS) and TCD detector in combination with Eager 200 or DP 200 were used.

Milling. The polymers were milled before using in a SM 2000 - mill of Retsch GmbH, Germany.

Drying. All materials were dried at 130°C in vacuum for 7 h over a molecular sieve.

Pyrolysis. The samples were heated between 300 and 750°C in 50°C-steps for 30 min each and at 750°C for 2 h.

DSC and TGA. Measurements of the materials were performed with TA Instruments DSC Q 1000 and TGA 500. The thermal behavior of the produced materials was examined in a temperature range of −50–350°C for DSC and −50–550°C for TGA. The rate for heating and cooling was 10 K min^{-1}.

Rheology. Dynamic shear measurements were performed using Advanced Rheometric Expansion System (ARES, TA Instruments, USA) using parallel plate geometry (25 mm diameter and 1 mm gap). All samples were tested at 235°C, after drying at 130°C, under nitrogen atmosphere to prevent oxidation of the specimens. Dynamic frequency sweep measurements were performed in the frequency range from 0.1 to 70 s^{-1} using strain amplitude within the linear viscoelastic regime.

Viscometry. The relative solution viscosity was determined by the viscosimeter device AVS 250 and the temperature-controlling device CT 1450 of the Schott Geräte GmbH, Germany. Thus, 100 mg dry polyester samples were weighed and dissolved under heating in the solvent. The solvent used was a mixture of phenol and 1.2-dichlorobenzene with a weight ratio of 3 : 2. The relative viscosity is determined at 25.0°C as a quotient η_{rel} of absolute viscosity (retention time) of the polymer solution η (t) and of the pure solvent η_0 (t_0) in an Ubbelohde viscometer; η_{spec} is defined by $\eta_{rel} - 1$. The single-point Eq. (1)[49] fits the experimental intrinsic viscosity [η] data best.

$$[\eta] =](1 + 4k_H\eta_{spec})^{0.5} - 1]/(2k_Hc) \quad (1)$$

The concentrations c of the polymer solutions of the composite samples were corrected with regard to the experimental amounts of clay components. The constant k_H is the Huggins constant with a value of = 0.25 ± 0.07 for the used solvent system.

The mathematical translation of the [η]DCB-values of PTT, analyzed in the solvent system *o*-dichlorobenzene/phenol (DCB), to the solvent system tetrachloroethane/phenol (TCE) described in Ref. 32 was performed using Eq. (2) (Kelsey et al.[50]).

$$IV_{TCE} = (IV_{DCB} - 0.036)/0.963 \quad (2)$$

Mass Spectroscopy. Electron-impact mass spectra (EI-MS) were taken on a MAT 711 spectrometer (Varian MAT, Bremen). The samples were analyzed between room temperature and 350°C and bombarded with electrons of energy of 80 eV.

Mechanical Testing. Tensile strength and modulus of the composites were measured according to DIN EN ISO 527 and 178, respectively, with a universal testing machine (Zwick 020) using the injection-molded standard test specimen. However, the tensile modulus was determined as the maximum derivative at the beginning of the stress–strain curve measured at 50 mm min^{-1} testing speed.

X-ray. X-ray diffraction (XRD) patterns were obtained using a Bruker-AXS D5000 X-ray diffractometer (40 kV, 30 mA) equipped with a Cu Kα radiation source (λ = 0.15406 nm) and a Ge(111) crystal monochromator. Scans were performed in symmetrical transmission technique in a 2Θ-range between 3° and 10° and a step size of 0.05° using 50 s for every step. The measured diffraction pattern were corrected with regard to parasitic scattering, absorption and polarization effects and normalized to electron units. The $d_{(001)}$ spacings were calculated from the 2Θ values.

Scanning Electron Microscopy (SEM) and EDX. A scanning electron microscope JSM 6330F (Jeol, Japan) was used at an acceleration voltage of 5 kV to study the morphology of sample cross sections. The cross sections were prepared by cryo-fracturing in liquid Nitrogen or with a rotating microtome (Leica RM 2255, Germany). The cut surfaces were further treated 3 min with an oxygen-plasma at 10^{-2} mbar in a MED010 (Balzers, Germany) to etch the polymer matrix from the surface and to expose the embedded nanoparticles completely. Finally, the surfaces were sputtered with a Platinum-layer (thickness 4 nm) to avoid electrical charging by the electron beam.

Transmission Electron Microscopy (TEM). The morphology of ultra thin cuts was studied with a transmission electron microscope CM 200 (Philips, Netherlands) at an acceleration voltage of 120 kV. The micrographs were taken with a digital camera MegaView II (Olympus, Germany). Ultra thin cuts (thickness ~ 60 nm) were prepared with an UltraCut S (Leica, Germany). The samples were cut at −100°C with a diamond blade and finally deposited onto a foliated copper mesh (50 μm).

RESULTS AND DISCUSSION

Solid-State-Polymerization

Preparation and Kinetic Investigations. PTT was treated under the conditions of solid-state polymerization at temperatures of 190, 200, and 210°C. The initial intrinsic viscosity of the PTT-sample was higher, IV = 0.964 dL g^{-1}, than such as those investigated by Duh (0.445–0.660 dL g^{-1}) and in the same order of magnitude as the sample applied by Kim (0.930 dL g^{-1}). Figure 1 presents the buildup curves of the intrinsic viscosities of PTT at different temperatures.

The influence of the processing temperatures on the kinetics of these SSP-reactions is clearly pronounced by the changed shapes of the curves and the graduated IV-values at comparable reaction times. An enhancement of IV from IV = 0.964–1.804 dL g^{-1} could be achieved for PTT(SSP) treated at 210°C for 30 h. Furthermore, this means an enhancement of nearly

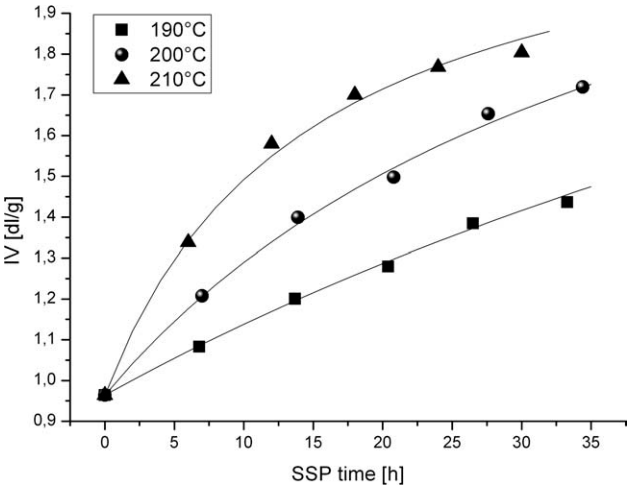

Figure 1. Buildup curves for SSP of PTT, treated under the conditions of SSP at $T = 190$, 200, and 210°C.

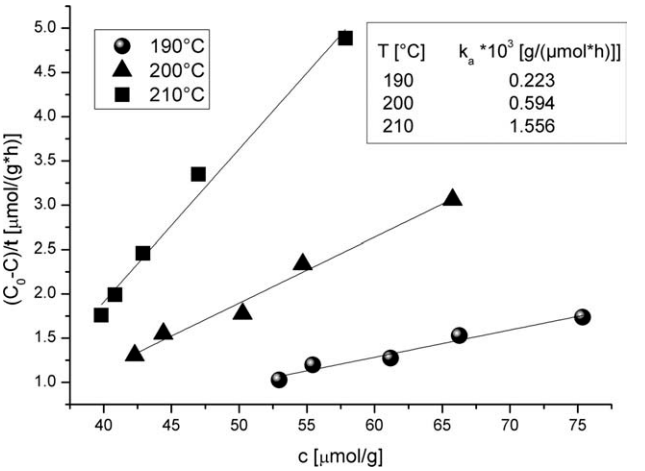

Figure 3. Linear plots according to Ref. 32 for the PTT(SSP)-samples treated at 190, 200, and 210°C.

12%, with respect to the highest IV-value presented by Kim et al. (IV = 1.613 dL g^{-1}).[27]

The magnitude of this effect was confirmed by the differences in melt viscosity of the educt, PTT, and the product PTT(SSP, 210°C, and 30 h). Figure 2 presents the melt viscosities of both polymers analyzed by frequency sweeps at 235°C.

The gain in melt viscosity of the PTT(SSP)-sample, expressed by the ratio of the melt viscosities at the frequency of 0.1 Hz, is 36. This increased viscosity is likely to support the clay exfoliation at the beginning of the extrusion process.

The data shown in Figure 1 can be analyzed according to the kinetic model presented by Duh[32] (Figure 3).

Reaction rate constants were calculated from slopes and intercepts based on these linear graphs (Figure 3).

An apparent activation energy of $E_a = 181$ kJ mol^{-1} and a frequency factor of $A_0 = 5.2 \times 10^{16}$ g (μmol h^{-1})$^{-1}$ were determined from the slope and the intercept of the corresponding Arrhenius-plot, respectively (Figure 4).

The apparent activation energy is higher than the reference data from the literature ($E_a = 108$ kJ mol^{-1}).[27,32] The comparably long reaction time we needed to prepare the high-molecular PTT(SSP) can be assumed as the main reason for the differences. Following the mathematical procedure described in Ref. 32 one can see that the reaction rate constants become comparably small. Furthermore, there are bigger differences between them, with respect to the reaction temperatures. This culminates in a bigger slope of the Arrhenius plot and, finally, in a higher apparent activation energy.

Isolated By-Products. During SSP the formation of a white sublimate was observed. Such by-products result from cyclic depolymerization reactions over a long period of time. By mass-spectroscopy, examined in a temperature range between 200 and 350°C, cyclic oligomers with different ring sizes n were identified (Table I).

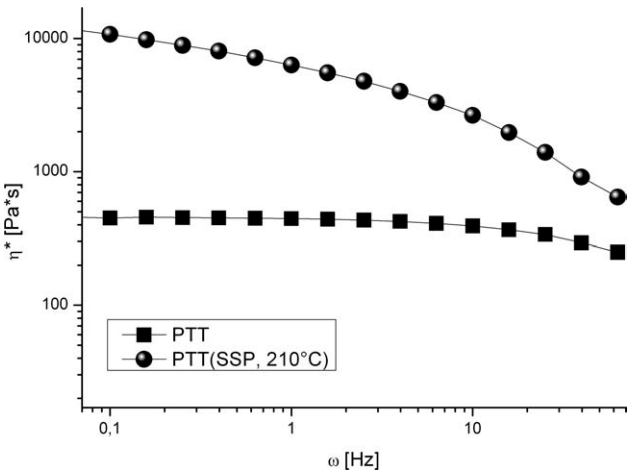

Figure 2. Melt viscosities of the polymers PTT and PTT(SSP, 210°C, 30 h), $T = 235$°C.

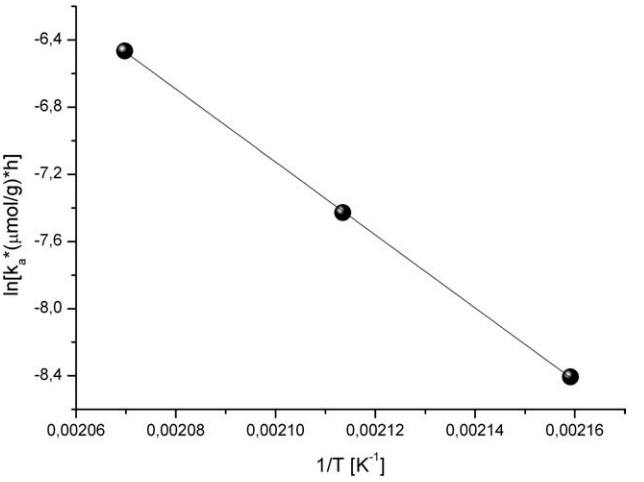

Figure 4. Arrhenius plot of the SSP-reactions of PTT, performed at 190, 200, and 210°C.

Table I. Molecular Ion and Ring Sizes of the Cyclic Oligomers, Formed During SSP of PTT

M/z	*n*
412	2
618	3
824	4
1030	5

The di-, tri-, tetra-, and pentamers were detected with a dominance of intensity for the dimer. The cyclic oligomers with larger rings, especially the tetra- and pentamer, could be found in traces only after drastic amplification. This trend is in accordance with the basic laws of ring formation in chemistry.

Thermoplastic Processing. All PTT(SSP)-samples were manufactured by injection molding, Table II presents the results of tensile tests.

Compared with non-pretreated PTT all PTT(SSP)-samples tend to show improvements in tensile strength (~ 2 MPa) and Young's modulus (about 200 MPa). The polymers are less elastic. With regard to the property improvements, there is no graduation in dependence on the SSP-temperatures between 190 and 210°C.

PTT(SSP)-Based Nanocomposites

Composite Preparation. PTT(SSP) prepared at 210°C was extruded with an OMC, modified with benzyldimethylstearylammonium cations, to manufacture composites with 3% of inorganic clay material. Based on the results of the first series of experiments,[47] extrusion was performed at 200 and 400 rpm. The experimental contents of inorganic fillers in the composites, examined by pyrolysis, are presented in Table III.

The percentages of the fillers are in a range between 2.8 and 3.3%. Differences with regard to the expected value of 3% can be explained by partial separation between the PTT(SSP)-powder and the filler in the storage container of the extruder.

Thermoanalytical Characterization. Characteristic results of DSC-studies of the PTT(SSP)-based materials were examined and are presented in Table IV.

The melting temperatures of the PTT(SSP)-samples increased slightly by ~ 1–2°C. The crystallization temperatures (T_c) shifted from 159 to 191–192°C. This means a decrease for ΔT ($T_m - T_c$) from 65 K [neat PTT(SSP)] to 33–35 K. Usually the lower ΔT predicts higher nucleation and crystallization rates.[51]

From the exothermic heat of fusion ΔH, the area enclosed between an exothermic curve and the base line, the crystalline degree is calculated according to Eq. (3):

Table II. Results of Tensile Tests of Neat PTT(SSP) Samples

Polymer		σ_{max} (MPa)	ε_{max} (%)	*E* (MPa)
PTT	Untreated	60.5 ± 0.5	6.4 ± 0.6	2080 ± 50
	190°C	62.6 ± 0.4	5.0 ± 2.0	2270 ± 20
	200°C	62.2 ± 0.1	3.9 ± 0.1	2280 ± 10
	210°C	62.4 ± 0.7	3.9 ± 0.1	2290 ± 30

Table III. Content of Clay-Materials in the Composites Made from PTT(SSP)

	PTT (SSP)
	Clay
200 rpm	3.3
400 rpm	2.8

$$X_C[\%] = (\Delta H/(\Delta H_0(1-\varphi)))100\% \quad (3)$$

where ΔH_0 is the fusion heat of fully crystalline polymer and φ means part of the inorganic filler. The ΔH_0 value adopted for PTT was 145.63 J g^{-1}, which was obtained by the conversion of 30 kJ mol^{-1}.[52] The PTT(SSP)-based composites show slightly higher degrees of crystallinity than the corresponding PTT-based samples. This could be a first indication for the support of composite formation, exfoliation for instance, by the high-molecular PTT(SSP).

Viscometry. To confirm this assumption Table V points out the effects of polymer degradation during processing by the intrinsic viscosities of the composite's matrix polymers.

Compared with the reference value $IV_{PTT(SSP)}$, there is a drop of intrinsic viscosity of the extruded SSP-based composites. The gain in molecular weight of PTT, enabled by the application of the SSP-procedure, was partially lost during extrusion. Reasons for degradation are on the one hand thermal degradation amplified by mechanical stress during processing. On the other hand, chemical degradation of the polyester can be attributed to reactions with decomposition products of the organic modifier of OMC. Nevertheless, the remaining IV-level of the PTT(SSP)-based composites was higher than the values of the corresponding samples prepared with non-pretreated PTT. Therefore, support of exfoliation by higher melt viscosity could be possible.

X-ray Analysis. The effectiveness of the SSP-treated PTT on exfoliation of the modified clay during melt processing was additionally examined by X-ray analysis. Figure 5 presents the WAXD-patterns of neat PTT, a mixture of modified clay (3%) and virgin PTT and the composites PTT/clay/200 rpm and PTT(SSP)/clay/200 rpm. The peak of the untreated modified clay is labeled by the corresponding *d*(001)-reflection.

For both composites prepared with either PTT or PTT(SSP), the WAXD-patterns are nearly congruent. The comparable efficiency of both polymers in this case can be interpreted in terms of the reduced melt viscosity of PTT(SSP), performed during processing by partial degradation (see Table V). The modified clay was mainly dispersed. A weak signal at $2\Theta = 5.2°$ ($d = 1.69$ nm) indicates a small part of remaining filler with a reduced final interlayer distance. As a reason for this effect, migration of the surfactant out of the filer galleries can be taken into consideration.[43] In comparison, the slightly increased crystalline degrees, analyzed by DSC, should be interpreted as a minor effect.

Mechanical Properties. Mechanical tests indicate a positive effect of PTT(SSP) on tensile strength and Young's modulus (Table VI).

Table IV. Selected DSC-Results of PTT, PTT(SSP), and the Corresponding Composites

Sample	T_m (°C)	ΔH_f (J g^{-1})	T_C (°C)	ΔH_C (J g^{-1})	ΔT (K)	X_C (%)
PTT(SSP)	224	73	159	59	65	40
PTT(SSP)/clay/200 rpm	226	59	191	66	35	45
PTT(SSP)/clay/400 rpm	225	62	192	67	33	46
PTT	223	73	157	53	66	36
PTT/clay/200 rpm	224	60	184	57	39	39
PTT/clay/400 rpm	223	66	185	62	38	42

T_m, ΔH_f, T_C, ΔH_C, ΔT, and X_C; 10 K min^{-1}, second scan.

The composite made from PTT(SSP) and modified clay, extruded at 200 rpm, shows the best results. Compared with the data of neat PTT(SSP) this means an increase in tensile strength of ~ 5% in combination with an enhancement of Young's modulus from 2290 to 2910 MPa (27%). The results of these experiments have to be compared with the mechanical properties of the corresponding PTT-based composites published in Ref. [47] (Table VI). Tensile strength of the samples was improved from 54–57 MPa (PTT-based) to 64–65 MPa (PTT(SSP)-based), this means a gain of 14–18%. Material stiffness increased from 2810 MPa (PTT-based) to 2910 MPa (PTT(SSP)-based) and from 2760 MPa (PTT-based) to 2790 MPa (PTT(SSP)-based) for speeds of rotation of 200 and 400 rpm, respectively. Elasticity changed only slightly without a remarkable effect.

The improved tensile strength of the PTT(SSP)-based composite, processed at 200 rpm, seems to be possible by the application of the high-molecular PTT(SSP). The degree of exfoliation of both composites (PPT- and PTT(SSP)-based) is comparable (Figure 5). Differences in the degrees of crystallinity are marginal with a small benefit for the PTT(SSP)-sample (Table IV) and the intrinsic viscosities of the PTT(SSP)-based composites are higher than the IV of the corresponding PTT-samples, independent the processing conditions (Table V). Therefore, the exfoliated platelets and the high-molecular matrix polymer seem to influence each other positively. This could mean a more homogeneous distribution of both the exfoliated and not exfoliated nanofiller fractions in the composite matrix (Figure 5), in combination with the marginal higher degree of crystallinity. Figure 7(a) presents a section of the distributed platelets in the PTT(SSP)-matrix. The pattern looks like an interpenetrating network. The more homogeneous the platelets are distributed the better should be the mechanical performance of the composites. Further investigations of particle distribution with respect to the molecular weight of the matrix are in preparation.

Table V. Intrinsic Viscosities (dL g^{-1}) of PTT- and PTT(SSP)-Based Materials

Samples	0 rpm	200 rpm	400 rpm
$IV_{PTT(SSP)}$ (dL g^{-1})	1.773	1.542	1.381
$IV_{PTT(SSP)/clay}$ (dL g^{-1})	-	1.314	1.081
IV_{PTT} (dL g^{-1})*	0.977	0.969	0.921
$IV_{PTT/clay}$ (dL g^{-1})*	-	0.895	0.834

Morphological Investigations. Cutting of PTT(SSP)/clay/200 rpm in preparation for TEM-imaging proved difficult. The mechanical forces during sample preparation seem to influence the shape of the composite layers. Figure 6 presents a typical TEM-micrograph of this nanocomposite.

Exfoliated platelets can be identified partially in combination with small agglomerates showing a parallel orientation. In addition to ultra thin cuts for TEM investigations surfaces of the composites were prepared by plasma etching for SEM-studies. Both, the outer surface and the cross section of the samples were investigated, where the cross section was prepared by cryo fracturing with subsequent planning with a microtome (RM2255, Leica). This technique avoids artifacts which can be induced by the mechanical impact of the blade in ultra thin cuts. The plasma etching was tested as a kind of "contactless" removal of the polymer matrix around the fillers on the surface of the nanocomposite samples. After plasma etching for 1 min the nanofiller platelets were laid bare from the polymer matrix [Figure 7(A)].

Compared with a SEM-micrograph of the pure modified clay [Figure 7(B)], the filler particles in the nanocomposites look like exfoliated platelets, however reduced in their size.

To identify the origin of the particles in Figure 7(A), the elemental compositions were studied by X-ray microanalysis

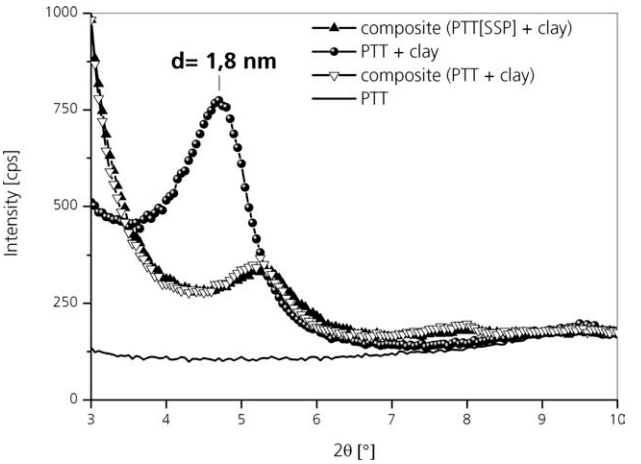

Figure 5. WAXD-patterns of PTT, a mixture of modified clay (3%) and virgin PTT and the composites PTT/clay/200 rpm and PTT(SSP)/clay/200 rpm.

Table VI. Selected Mechanical Properties of Composites Prepared with PTT(SSP), Together with the Data of the Corresponding PTT-Samples.[47]

Samples	σ_{max} (MPa)	ε_{max} (%)	*E* (MPa)
PTT(SSP)	62.4 ± 0.9	3.9 ± 0.1	2290 ± 30
PTT(SSP)/3%clay/200 rpm	65.6 ± 0.6	2.7 ± 0.1	2910 ± 20
PTT(SSP)/3%clay/400 rpm	63.8 ± 0.7	2.6 ± 0.1	2790 ± 10
PTT	60.5 ± 0.5	6.4 ± 0.6	2080 ± 50
PTT/3%clay/200 rpm	57.6 ± 2.5	2.3 ± 0.2	2810 ± 20
PTT/3%clay/400 rpm	54.2 ± 1.7	2.2 ± 0.1	2760 ± 30

(EDX, Thermo Electron, US). The spectra of virgin clay and the etched particles, Figure 8(A,B), respectively, show a similar elemental content. The obviously high values for carbon are due to the embedding of the platelets in the carbon rich PTT matrix. The platinum peak is produced by the sputtered layer at the flat surface. But the equivalent ratio between Si and Al intensities prove the etched particles to be the nanofiller platelets.

Furthermore, an orientation effect of the filler platelets was detected. In a surface layer, the platelets are oriented parallel to the sample surface while in the inner region the orientation is random. This is demonstrated in Figure 9. In region A, the samples surface itself is shown. Region B is the outer part of the fracture surface, i.e., near the sample surface and shows the preferred orientation of the platelets. In the inner region C, on the other hand, no preferred orientation can be seen. The region B layer thickness varies between 0.5 and 3 μm. These features indicate an orientation mechanism induced by the flow of the polymer melt into the molding tool of the injection molding machine. Regardless of their nanodimensions, the orientation behavior of the filler platelets is very similar to the orientation of short cut fibers during injection molding processes, for instance.[53]

The fracture cross-section of SSP-PTT shows polygonal areas with a pit-like surface pattern after plasma etching [Figure 10(A)].This structure was also detected in between the filler particles of the corresponding composites and indicates remaining polymer matrix [Figure 10(B)].

SSP of a Composite Made from Pristine PTT and Modified Clay Extruded at 200 rpm [PTT/clay/200 rpm (SSP)]

To complete the concept of these experiments, composite-pellets made from PTT and modified clay were posttreated at 210°C

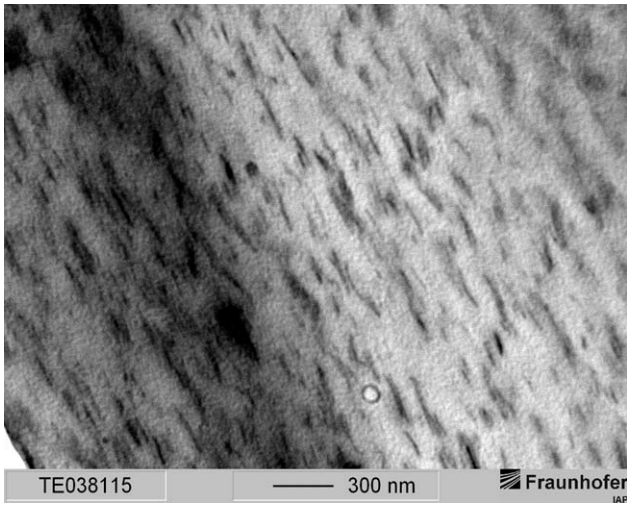

Figure 6. TEM-micrograph of PTT(SSP)/clay/200 rpm.

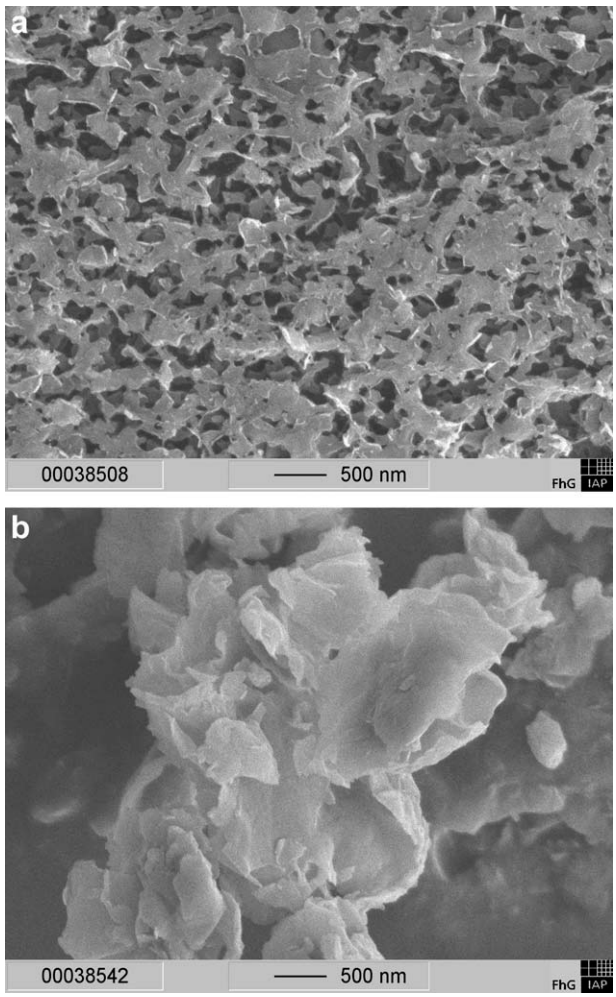

Figure 7. SEM-micrograph of the surface of plasma etched PTT(SSP)/clay/200 rpm (A), and of pure modified clay particles (B).

Applied Polymer SCIENCE

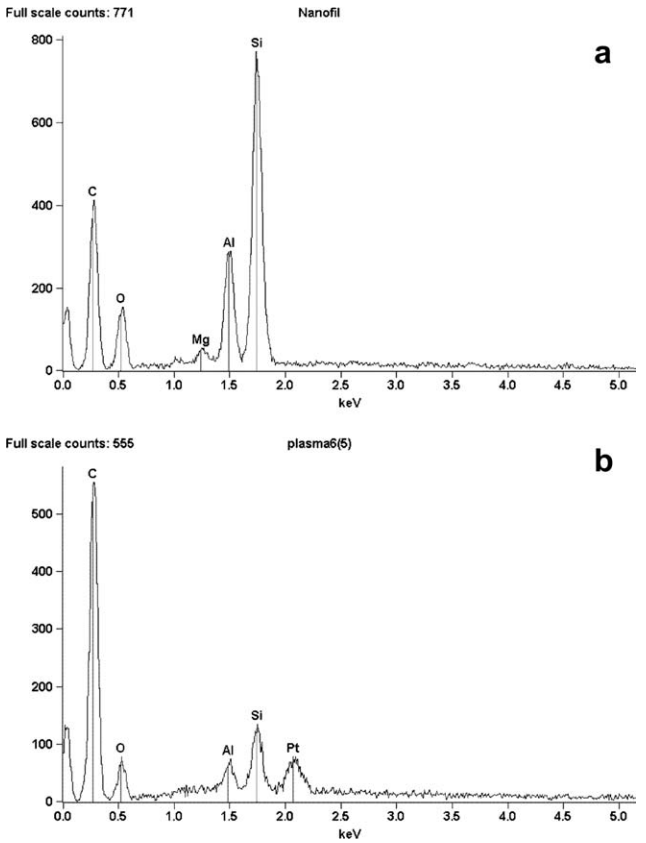

Figure 8. EDX-spectra of pure modified clay (A) and platelets in PTT(SSP)/clay/200 rpm after plasma etching (B).

under the same conditions of solid-state-polymerization as used for the pristine PTT and finally characterized. Table VII presents the results of tensile tests.

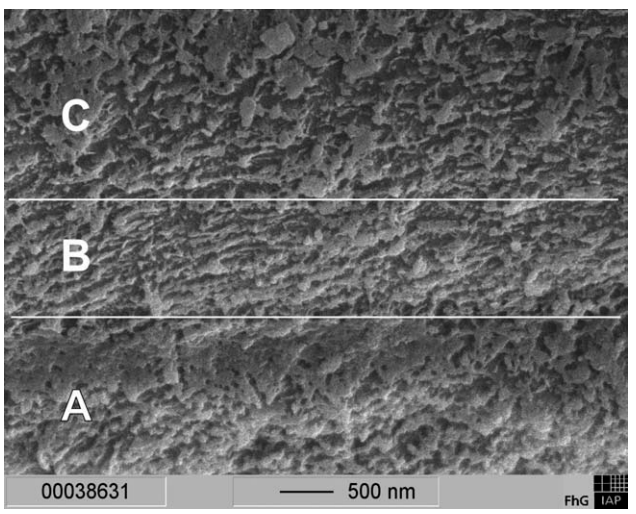

Figure 9. SEM-micrograph of the cross section surface of plasma etched PTT(SSP)/clay/200 rpm: (A) sample surface, (B) outer region with platelets oriented parallel to the sample surface, (C) random orientation of platelets in the inner region.

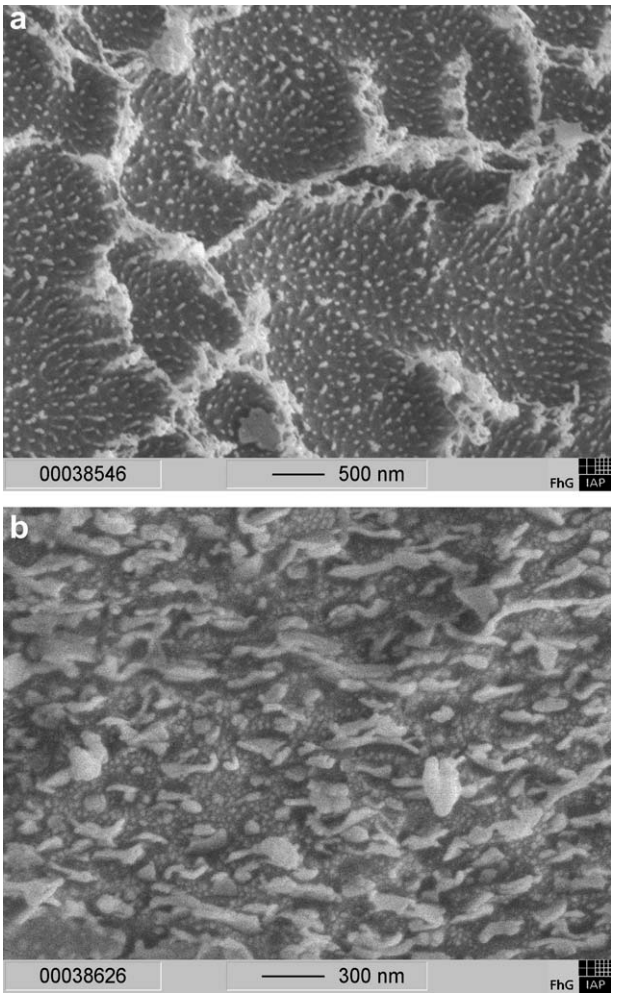

Figure 10. Pit-like pattern of the plasma-etched surface of a neat SSP-PTT-sample (A) and between the corresponding nanofiller platelets (B).

The presence of the modified clay in the composite suppressed the success of solid-state-polymerization for neat PTT. While modulus is of the same order of magnitude, tensile strength broke down to half of the initial value. The matrix of the processes composite was characterized by an intrinsic viscosity of IV = 0.538 dL g^{-1}, clearly smaller than that of the educt sample (Table V). Experiments with aromatic polyesters like PET and MMT show accelerating effects for the SSP-kinetic.[54] The

Table VII. Results of Tensile Tests of PTT, PTT/clay/200 rpm and PTT/clay/200 rpm Handled Under the Conditions of SSP [PTT/clay/200 rpm (SSP)]

	PTT	PTT/clay/200 rpm	PTT/clay/200 rpm (SSP)
σ_{max} (MPa)	60.5 ± 0.5	57.6 ± 2.5	31 ± 4
ε_{max} (%)	6.4 ± 0.6	2.3 ± 0.2	1.1 ± 0.2
E (MPa)	2080 ± 50	2810 ± 20	2880 ± 30

organically modified clay used in our experiments is modified with benzyltrialkylammonium cations. Degradation of the polyesters initiated by the modified nanofiller can be attributed to the modifier's structure. Thermal degradation of such organic compounds results in fragmentation reactions.[55] Their decomposition products depend on the structure of the ammonium cation's substituents. In the case of benzyl groups, bond cleavage is preferred due to resonance stabilization effects of the aromatic ring.[56] With respect to Hofmann degradation tertiary amines have to be expected.[57] Such decomposition products are highly reactive, especially under the processing conditions used. Amines can support polymer degradation due to their high basicity.[58]

Besides the chemical aggressiveness of the modified filler under the conditions of long-term SSP-experiments, the hindered diffusion of volatile reaction by-products out of the polymer pellets during SSP due to the presence of partially exfoliated clay could be another reason for degradation of the matrix polymer. If the organic modifier degrades thermally then partial agglomeration of filler components during injection molding cannot be excluded. Agglomerates could act as defects with negative consequences for tensile strength.

CONCLUSIONS

PTT was successfully subjected to solid-state-polymerization (SSP) at different temperatures to adapt melt viscosity by an increased average molecular weight to the conditions of nanocomposite preparation. Based on the kinetic model for SSP-Reactions,[32] a comparably high apparent activation energy of E_a = 180.6 kJ mol^{-1} was estimated. The higher value compared to[27,32] ($\sim$ 108 kJ/mol) can be explained by the longer reaction time need to prepare the very high-molecular PTT(SSP). The sublimate produced during SSP could be identified as a mixture of cyclic oligomers based on 2, 3, 4, and 5 monomeric units. The success of SSP was evidenced by the improvement in intrinsic viscosity of $\sim$ 83% after polycondenzation at 210°C for 30 h. Additionally, the mechanical properties of neat PTT(SSP) were improved by an increase of tensile strength from 60.5 to 62.5 MPa and an enhancement of Young's modulus from 2080 to 2290 MPa. PTT(SSP) becomes partially degraded during extrusion to manufacture the corresponding composites. In this case the typical graduation with rising speeds of rotation was observed, too. The partially degraded PTT(SSP) showed higher molecular weight than the manufactured PTT. PTT(SSP) supported the process of composite formation. Compared with PTT/clay/200 rpm tensile strength of PTT(SSP)/clay/200 rpm raised from σ = 57.6 MPa to σ = 65.6 MPa (13.9%) and Young's modulus was enhanced from E = 2810–2910 MPa. Change of elongation was comparable for both composites. Filler platelets in the PTT(SSP)-matrix were visualized by SEM of especially plasma-etched sample surfaces. Exfoliation was partially successful, in accordance with WAXD-analysis, the contact between filler and matrix seems to be weak. By SSP-processing of the composite PTT/clay/200rpm according to the used SSP-method a drastic loss of tensile strength was detected, breaking the mechanical properties down to a useless level. The conditions of this solid-state-polymerization stimulated degradation of the matrix polymer PTT by thermal energy and chemical actions of partially decomposed organic modifier of the nanofiller.

ACKNOWLEDGMENTS

The authors thank Dr. A. Holländer, head of surface-group, Fraunhofer Institute for Applied Polymer Research (IAP), for the realization of plasma etching experiments. They are grateful to Dr. G. Holzmann, former head of mass spectrometry, Institut für Chemie und Biochemie, Freie Universität Berlin, for performing the mass-spectroscopy experiments.

REFERENCES

1. Cho, H. W.; Lee, J. S.; Prabu, A. A.; Kim, K. J. *Polym. Compos.* **2008,** *29*, 1328.
2. Ray, S. S.; Okamoto, M. *Prog. Polym. Sci.* **2003,** *28*, 1539.
3. Ray, S. S.; Bousmina, M. *Prog. Mater. Sci.* **2005,** *50*, 962.
4. Ray, S. S.; Okamoto, K.; Yamada, K.; Okamoto, M. *Nano Lett.* **2002,** *2*, 423.
5. Maiti, P.; Batt, C. A.; Giannelis, E. P. *Polym. Mater. Sci. Eng.* **2003,** *88*, 58.
6. Park, H. M.; Li, X.; Chang-Zhu, J.; Park, C. Y.; Cho, W. J.; Ha, C. K. *Macromol. Mater. Eng.* **2002,** *287*, 553.
7. Kojima, Y.; Usuki, A.; Kawasumi, M.; Fukushima, Y.; Okada, A.; Kurauchi, T.; Kamigaito, O. *J. Mater. Res.* **1993,** *8*, 1179.
8. Kato, M.; Usuki, A.; Okada, A. *J. Appl. Polym. Sci.* **1997,** *66*, 1781.
9. Rong, J.; Jing, J.; Li, H.; Sheng, M. A. *Macromol. Rapid Commun.* **2001,** *22*, 329.
10. Bourbigot, S.; Vanderhart, D. L.; Gilman, J. W.; Awad, W. H.; Davis, R. D.; Morgan, A. B.; Wilkie, C. A. *J. Polym. Sci. B Polym. Phys.* **2003,** *41*, 3188.
11. Huang, X.; Lewis, S.; Brittain, W. J.; Vaia, R. A. *Macromolecules* **2000,** *33*, 2000.
12. Hasegawa, N.; Okamoto, H.; Kato, M.; Usuki, A.; Sato, N. *Polymer* **2003,** *44*, 2933.
13. Wang, Z.; Pinnavaia, T. *J. Chem. Mater.* **1998,** *10*, 3769.
14. Zhanga, G.; Shichia, T.; Takagi, K. *Mater. Lett.* **2003,** *57*, 1858.
15. Wu, D.; Zhou, C.; Zhang, M. *J. Appl. Polym. Sci.* **2006,** *102*, 3628.
16. Chang, J.-H.; Kim, S. J.; Im, S. *Polymer* **2004,** *45*, 5171.
17. Glenz, W. *Kunststoffe* **2007,** *10*, 76.
18. Wijayathunga, V. N.; Lawrence, C. A.; Blackburn, R. S.; Bandara, M. P. U.; Lewis, E. L. V.; El-Dessouky, H. M.; Cheung, V. *Opt. Laser. Technol.* **2007,** *39*, 1301.
19. Eipper, A. *Kunststsoffe* **2007,** *10*, 120.
20. Chuah, H. H. Paper presented at Tifcon '96', The Textile Institute, Blackpool, UK, Nov. 6, **1996.**
21. Kurian, J. V. *J. Polym. Environ.* **2005,** *13*, 159.
22. Bhatia, K. K. US Pat. 5,599,900, **1997.**
23. Kelsey, D. R. US Pat. 6,093,786, **2000.**
24. Duh, B. US Pat. 6,297,315, **2001.**

25. Kim, T.-K.; Son, Y.-A.; Lim, Y.-J. *Dyes Pigm.* **2005,** *67*, 229.
26. Chen, K.; Tang, X. *J. Appl. Polym. Sci.* **2004,** *91*, 1967.
27. Kim, S. H.; Kim, J. H. *Fibers Polym.* **2010,** *11*, 170.
28. Karayannidis, G. P.; Sideridou, I.; Zamboulis, D.; Stalidis, G.; Bikiaris, D.; Lazaridis, N.; Wilmes, A. *Angew. Makromol. Chem.* **1991,** *192*, 155.
29. Wu, D. *Macromolecules* **1997,** *30*, 6737.
30. Duh, B. *J. Appl. Polym. Sci.* **2002,** *84*, 857.
31. Chang, T. M. *Polym. Eng. Sci.* **1970,** *10*, 364.
32. Duh, B. *J. Appl. Polym. Sci.* **2003,** *89*, 3188.
33. Liu, W.; Mohanty, A. K.; Drzal, L. T.; Misra, M.; Kurian, J. V.; Miller, R. W.; Strickland, N. *Ind. Eng. Chem. Res.* **2005,** *44*, 857.
34. Run, M.; Song, H.; Wang, S.; Bai, L.; Jia, Y. *Polym. Compos.* **2009,** *30*, 87.
35. Wu, C.-S. *J. Appl. Polym. Sci.* **2009,** *114*, 1633.
36. Russo, G. M.; Simon, G. P.; Incarnato, L. *Macromolecules* **2006,** *39*, 3855.
37. Kim, J. Y.; Han, S. I.; Hong, S. *Polymer* **2008,** *49*, 3335.
38. Kim, N. H.; Malhotra, S. V.; Xanthos, M. *Microporous Mesoporous Mater.* **2006,** *96*, 29.
39. Fornes, T. D.; Yoon, P. J.; Hunter, D. L.; Keskkula, H.; Paul, D. R. *Polymer* **2002,** *43*, 5915.
40. Gilman, J. W.; Awad, W. H.; Davis, R. D.; Shields, J.; Harris, R. H., Jr.; Davis, C.; Morgan, A. B.; Sutto, T. E.; Callahan, J.; Trulove, P. C.; DeLong, H. C. *Chem. Mater.* **2002,** *14*, 3776.
41. Zhu, J.; Morgan, A. B.; Lamelas, F. J.; Wilkie, C. A. *Chem. Mater.* **2001,** *13*, 3774.
42. Vaia, R. A.; Teukolsky, R. K.; Giannelis, E. P. *Chem. Mater.* **1994,** *6*, 1017.
43. Gurmendi, U.; Eguiazabal, J. I.; Nazabal, J *Eur. Polym. J.* **2008,** *44*, 1686.
44. Suprakas, S. R. S. S.; Okamoto, M. *Prog. Polym. Sci.* **2003,** *28*, 1539.
45. Frounchi, M.; Dourbash, A. *Macromol. Mater. Eng.* **2009,** *294*, 68.
46. Scaffaro, R.; Botta, L.; Ceraulo, M.; La Mantia, F. P. *J. Appl. Polym. Sci.* **2011,** *122*, 384.
47. Engelmann, G.; Bonatz, E.; Ganster, J. *J. Appl. Polym. Sci. (accepted).*
48. Ramiro, J.; Eguiaza'bal, J. I.; Nazabal, J. *J. Appl. Polym. Sci.* **2002,** *86*, 2775.
49. Liu, Y. *Macromol. Mater. Eng.* **2001,** *286*, 611.
50. Kelsey, D. R.; Blackbourn, R. L.; Tomaskovic, R. S.; Reitz, H.; Seidel, E.; Wilhelm, F. US Pat. 6,277,947, **2001.**
51. Wunderlich, B. Macromolecular Physics; Academic Press: New York, **1976; Vol.** *2.*
52. Pyda, M.; Boller, A.; Grebowicz, J.; Chuah, H.; Lebedev, B. V.; Wunderlich, B. *J. Polym. Sci. B Polym. Phys.* **1998,** *36*, 2499.
53. Shokri, P.; Bhatnagar, N. *Polym. Compos.* **2007,** *28*, 214.
54. Yu, H.; Han, K.; Yu, M. *J. Appl. Polym. Sci.* **2004,** *94*, 971.
55. Xie, W.; Gao, Z.; Liu, K.; Pan, W.-P.; Vaia, R.; Hunter, D.; Singh, A. *Thermochim. Acta.* **2001,** *367*, 339.
56. Cervantes-Uc, J. M.; Cauich-Rodriguez, J. V.; Vázquez-Torres, H.; Garfias-Mesias, L. F.; Donald, R.; Paul, D. R. *Thermochim. Acta.* **2007,** *457*, 92.
57. Haskins, N. J.; Mitchell, R. *Analyst.* **1991,** *116*, 901.
58. Buxbaum, L. H. *Angew Chem Int Edit* **1968,** *7*, 182.